Supplementary Information

High-performance $LiMn_{1-x}Fe_xPO_4$/C cathode constructed by nano-sized spherical $MnFePO_4 \cdot H_2O$ precursor via scalable reverse-titration co-precipitation strategy

Hongwei Yang[a], Liuquan Hu[b], Zhuang Hu[a], Wentian Yi[a], Zhe Mu[a], Jie Wu[a], Zewei Xie[c], Changling Fan[a,d,*]

[a] *College of Materials Science and Engineering, Hunan University, Changsha, Hunan, 410082, China*

[b] *Minmetals New Energy Materials (Hunan) Co., Ltd., Changsha, Hunan, 410205, China*

[c] *Hunan Changyuan Lico New Energy Co., Ltd., Changsha, Hunan, 410205, China*

[d] *Hunan Province Key Laboratory for Advanced Carbon Materials and Applied Technology, Hunan University, Changsha, Hunan, 410082, China*

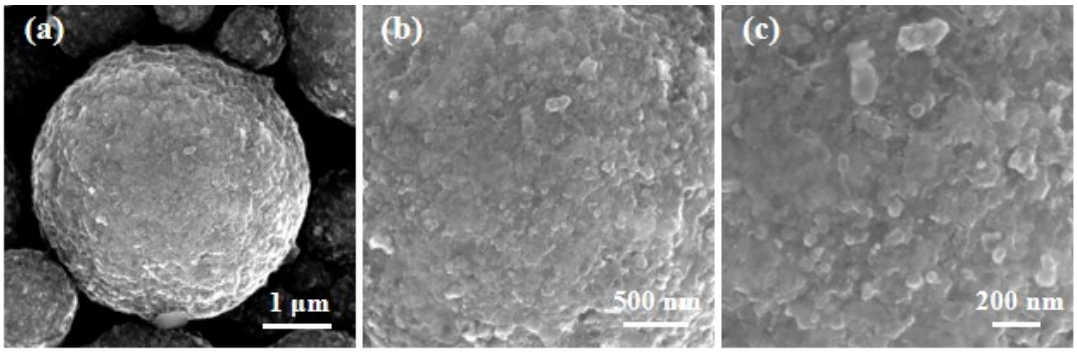

Figure S1. TEM image of the final L-SMSD material.

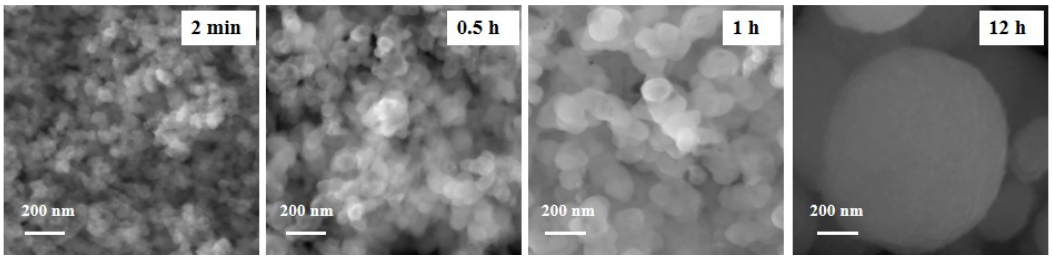

Figure S2. Time-resolved SEM images of $MnFePO_4 \cdot H_2O$ precursor at different reaction stages: (a) 2 min, (b) 0.5 h, (c) 1 h, and (d) 12 h.

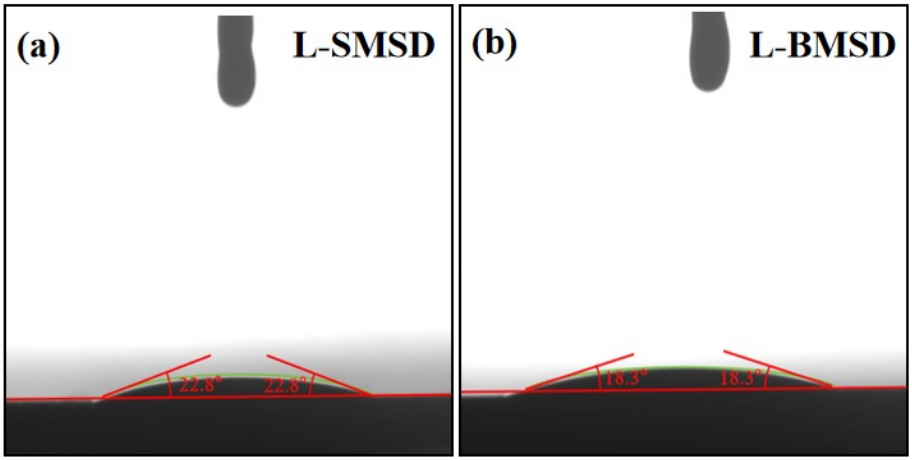

Figure S3. Contact angle optical images of electrolyte droplets on the surface of L-SMSD and L-BMSD cathode.

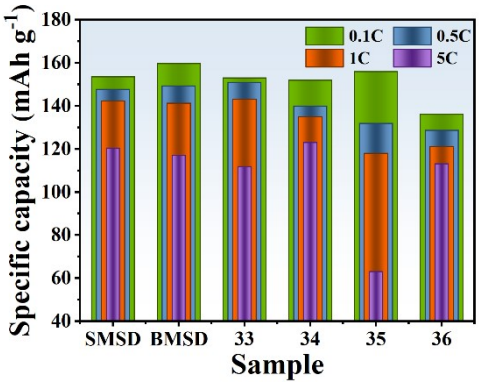

Figure S4. Comparison of half-cell rate capability with recently reported samples.

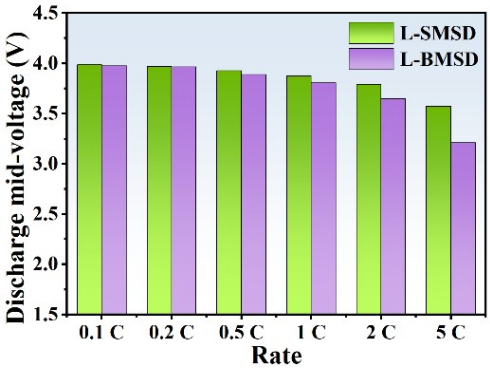

Figure S5. Comparison of half-cell discharge median voltage at different rates.

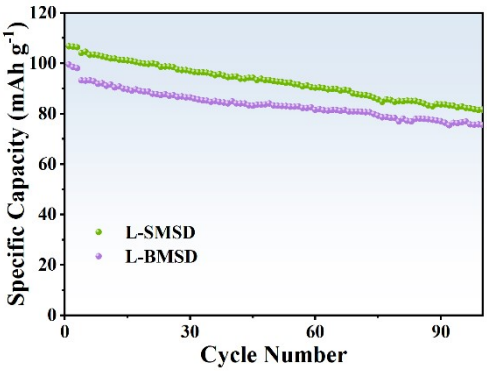

Figure S6. Cycling performance of graphite || $LiMn_{1-x}Fe_xPO_4$/C full cells at 1C over 100 cycles.

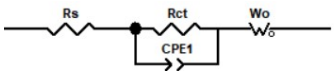

Figure S7. Equivalent circuit diagram for fitting the in-situ EIS data.

The components and their physical meanings are: (1) **Rs**: Ohmic resistance (electrolyte, current collector, cell connections). (2) **Rct // CPE1:** Charge transfer resistance and double-layer capacitance at the electrode/electrolyte interface. (3) **W_o:** Warburg impedance corresponding to solid-state Li^+ diffusion within the cathode material.

Table S1. Lattice parameters of $MnFePO_4 \cdot H_2O$ precursor.

Samples	*a* (Å)	*b* (Å)	*c* (Å)	*V* (Å^3)
$MnFePO_4 \cdot H_2O$	6.892	7.496	7.379	350.7
Standard PDF #97-006-2220	6.912	7.470	7.357	351.5

Table S2. Rietveld refinement results of L-BMSD sample. (Rwp = 6.280%, GOF = 1.98)

L-BMSD	Atom	x	y	z	Occ.
Atomic Occupancies	Li1	0.00000	0.00000	0.00000	0.9642
	Fe2	0.00000	0.00000	0.00000	0.0358
	Fe1	0.28236	0.25000	0.97188	0.6442
	Mn1	0.28236	0.25000	0.97188	0.3200
	Li2	0.28236	0.25000	0.97188	0.0358
	P1	0.09320	0.25000	0.40738	1.0000
	O1	0.09671	0.25000	0.73874	1.0000
	O2	0.45480	0.25000	0.20355	1.0000
	O3	0.16130	0.04700	0.28200	1.0000
Lattice Parameters		*a* (Å)	*b* (Å)	*c* (Å)	*V* (Å^3)
		10.40394	6.06834	4.72619	298.386

Table S3. Rietveld refinement results of L-SMSD sample. (Rwp = 6.295%, GOF = 2.14)

L-SMSD	Atom	x	y	z	Occ.
Atomic Occupancies	Li1	0.00000	0.00000	0.00000	0.9688
	Fe2	0.00000	0.00000	0.00000	0.0312
	Fe1	0.28333	0.25000	0.97040	0.6488
	Mn1	0.28333	0.25000	0.97040	0.3200
	Li2	0.28333	0.25000	0.97040	0.0312
	P1	0.09343	0.25000	0.41226	1.0000
	O1	0.09697	0.25000	0.74311	1.0000
	O2	0.45185	0.25000	0.19486	1.0000
	O3	0.16336	0.04761	0.29312	1.0000
Lattice Parameters		*a* (Å)	*b* (Å)	*c* (Å)	*V* (Å^3)
		10.39565	6.06425	4.72303	297.749

Table S4. Comparison of process efficiency and electrochemical performance between the present work and three reported references.

Comparison aspect	Ref.38	Ref.39	Ref.40	SMSD in this work
Material system	$LiFePO_4$/C	$LiFePO_4$/C	$LiFe_{0.25}Mn_{0.75}PO_4$/C	$LiMn_{0.68}Fe_{0.32}PO_4$/C
Grinding method	Sand milling	No milling	Ball + Sand milling	Sand milling
Total grinding time	6 h	none	4 h (3 h+1 h)	0.5 h
Spray drying time	Not used	45 min	Not specified	15 min
Particle size	200-800 nm	9 μm (D50)	~50 nm	4.806 μm (D50)
Specific capacity (mAh g^{-1})	150.3 (0.1C)	98.0 (0.1C)	148.4 (0.05C)	153.5 (0.1C)
Cycling stability	91.9% (200/1C)	59.7% (200/0.5C)	90.3% (100/1C)	95.2% (450/1C)

Note: For comparison, only carbon-coated samples are selected from each reference (excluding CNTs, graphene, or rGO modifications).

TEXT. S1. The rationale for the $KMnO_4$ dosage is as follows.

The amount of $KMnO_4$ was determined by considering its dual role as both the oxidant and an additional manganese source. In this system, $KMnO_4$ oxidizes Mn^{2+} from $MnSO_4$ and Fe^{2+} from $FeSO_4$ to their trivalent states. During this process, Mn^{7+} in MnO_4^- is reduced. Under the strongly oxidizing conditions of the reaction medium (pH = 1.7-2.0), the Mn species derived from $KMnO_4$ is ultimately incorporated into the precursor as Mn^{3+}. Therefore, all manganese atoms, regardless of whether they originate from $MnSO_4$ or $KMnO_4$, are incorporated into the final $MnFePO_4 \cdot H_2O$ precursor lattice as Mn^{3+}.

The reaction can be summarized as:

Step 1 (Oxidation):

$$MnO_4^- + 2.4Mn^{2+} + 1.6Fe^{2+} + 8H^+ \rightarrow 3.4Mn^{3+} + 1.6Fe^{3+} + 4H_2O$$

Step 2 (Precipitation):

$$3.4Mn^{3+} + 1.6Fe^{3+} + 5PO_4^{3-} \rightarrow 5Mn_{0.68}Fe_{0.32}PO_4$$

Accordingly, when the molar amount of $KMnO_4$ is set to one quarter of the total amount of $MnSO_4$ and $FeSO_4$, it provides not only sufficient oxidizing capacity for the conversion of Mn^{2+}/Fe^{2+} to Mn^{3+}/Fe^{3+}, but also the additional manganese necessary to achieve the final Mn:Fe ratio of 0.68:0.32 in the precursor.